Phys. Status Solidi B **247**, No. 5, 1039–1047 (2010) / **DOI** 10.1002/pssb.200945484

physica status solidi b
www.pss-b.com
basic solid state physics

Kinetic Monte Carlo study of self-organization of low-dimensional nanostructures on fcc (110) surfaces

Nikolay N. Negulyaev*[,1], Oleg V. Stepanyuk[2], Larissa Niebergall[3], and Alexander M. Saletsky[2]

[1] Fachbereich Physik, Martin-Luther-Universität, Halle-Wittenberg, Friedemann-Bach-Platz 6, 06099 Halle, Germany
[2] Faculty of Physics, Moscow State University, 119899 Moscow, Russia
[3] Max-Planck-Institut für Mikrostrukturphysik, Weinberg 2, 06120 Halle, Germany

Received 19 October 2009, accepted 22 December 2009
Published online 29 January 2010

PACS 61.46.−w, 81.07.Vb, 81.16.Dn

* Corresponding author: e-mail negulaev@mpi-halle.de, Phone: +49 345 5582975, Fax: +49 345 5511223

Performing large-scale atomic simulations by means of kinetic Monte Carlo method we study room temperature self-organization of 3d magnetic atoms (Fe, Co) on fcc (110) surfaces (Pd(110), Cu(110)) in the sub-monolayer regime. The energetics of various diffusion processes relevant for these systems is investigated based on first principles calculations. We reveal that surface-confined atomic intermixing plays a significant role in the formation of nanostructures. Our results lead to the conclusion that the deposited species (Fe, Co) are captured into the topmost surface layer, while the ad-layer structure consists mainly of the expelled substrate atoms (Pd, Cu). Our studies shed a light on recent experimental investigations on the metal-on-metal growth on fcc (110) surfaces.

1 Introduction During the last two decades novel materials have been widely studied due to the development of electronic, magnetic, and data storage devices [1]. The evolution of the surface science and the recent progress in ultra-high vacuum techniques have made the fabrication and the investigation of magnetic properties of atomic-scale materials (such as nanowires [2–12], nanostripes [6, 13–21], nanoclusters [22–30], and nanodots [17, 31–36]) a rather hot topic. One of the basic tools for the manufacturing of nanostructures on surfaces is the epitaxial growth – a method of depositing individual atoms on a crystalline substrate at high vacuum. Surface-confined atomic intermixing can play a crucial role in the formation of nanostructures on surfaces. During this process the deposited species are captured into the topmost substrate layer, while the ad-layer structure consists of substituted surface atoms.

Since the beginning of the 1990s, scientists have put a lot of efforts into detailed investigation of intermixing on surfaces. Surprisingly, a novel kind of stable 2D alloys has been discovered: it has been found that two elements, which are immiscible in the bulk, could form a mixture of atoms confined within the topmost substrate layer. It has been shown that generally, such surface-confined mixing arises in systems which are dominated by the atomic mismatch [37]. Mismatch renders the elements immiscible in the bulk, and confines the minority of species to the substrate, inhibiting them from segregating within the surface layer [37]. Up to now, numerous experimental and theoretical studies have examined the formation of surface alloys. On a (100) surface the interface intermixing in the sub-monolayer regime has been observed (or predicted in the theoretical calculations) for the following systems: Na/Al(100) [38], Au/Cu(100) [39], Ag/Cu(100) [40, 41], Rh/Ag(100) [42], Pd/Ag(100) [43], Cu/Ni(100) [44], Ni/Cu(100) [45, 46], Fe/Cu(100) [47, 48], Co/Cu(100) [49, 50], Au/Fe(100) [51], As/Si(100) [52], Ge/Si(100) [52, 53], Pt/Ge(100) [54, 55]. For a (111) substrate the interface intermixing has been discovered for Na/Al(111) [56, 57], K/Al(111) [38, 57], Ag/Pt(111) [58, 59], Sb/Ag(111) [60], Au/Ni(111) [61], Ge/Ag(111) [62], and Co/Cu(111) [63]. The same phenomenon has been also observed on a fcc (110) surface at thermal deposition (TD) of Au on Ni(110) [64] and Ag on Cu(110) [65].

An unreconstructed fcc (110) substrate is known to be an ideal template for the self-assembly of 1D and quasi-1D atomic structures [66]. This substrate consists of close-packed atomic rows oriented along the [1–10]

crystallographic direction and separated by deep channels [67]. Since the atomic diffusion is strongly anisotropic and takes place predominantly along the [1–10] direction, growth of linear chains, or nanoscale islands oriented parallel to the channels is expected. Indeed, self-organization of monatomic wires during deposition of Cu on Pd(110) [66, 68, 69] and Co on Pd(110) [6] has been observed. In other related systems, like Au/Ni(110) [64], Ag/Cu(110) [65], Co/Cu(110) [70, 71], formation of 2D nanoislands, elongated along the [1–10] direction, has been found in the sub-monolayer regime. As a rule, these experimental investigations have been performed at room temperature (RT) or close to it [69]. Theoretical calculations demonstrate that deposited species can exchange with surface atoms on a (110) surface with reasonably low activation barriers, which are operative at such temperatures [72–74]. This hints that atomic intermixing can play a crucial role in the interface formation during heteroepitaxy on fcc (110).

A detailed understanding of different growth regimes as a function of temperature T, deposition flux F, and coverage D, is possible only if diffusion barriers of the relevant atomic events are known. The progress in this direction for the case of homoepitaxy on a fcc (110) surface has been already achieved [75–78]. While an exhaustive theoretical knowledge about atomic processes driving the self-assembly of low-dimensional nanostructures during heteroepitaxial growth on fcc (110) is still missing. For some particular systems, like Au/Ni(110) [64], the total energy calculations have been performed. Molecular static calculations by means of embedded-atom method have been reported for Cu/Pd(110) [72]. Nevertheless no large-scale atomic simulations of the heteroepitaxial growth on fcc (110) based on the first principles studies has been performed until recently [79].

In this paper we demonstrate the dramatic effect of atomic intermixing on the atomic self-assembly during the early stages of the heteroepitaxial growth on a fcc (110) surface. We report on theoretical studies of RT TD of 3d magnetic atoms (Fe and Co) on two substrates, Pd(110) and Cu(110). Diffusion barriers of relevant atomic events are obtained based on density function theory (DFT) calculations. Kinetic Monte Carlo (kMC) simulations [80] are involved to reveal the structure of the interface at the atomic scale. Our results indicate that (i) atomic exchange between deposited and substrate atoms and (ii) surface diffusion of expelled substrate adatoms are the driving forces of atomic self-assembly on fcc (110).

The remainder of the paper has the following structure. In Section 2 we study RT heteroepitaxy of Fe and Co atoms on Pd(110). In Section 3 we perform large-scale atomic simulations of epitaxial growth of Co on Cu(110).

2 Fe and Co on Pd(110) In this section the growth scenario of atomic structures during RT epitaxy of 3d magnetic atoms (Fe and Co) on Pd(110) is discussed. First we present the results of DFT calculations of activation barriers of atomic events responsible for self-organization of 3d atoms on Pd(110). Next we perform large-scale atomic simulations by means of kMC method in order to demonstrate the interface structure in the examined systems. Further in this section we mainly concentrate on Fe atoms. Our studies demonstrate that the growth scenarios of Co and Fe on Pd(110) are qualitatively similar (see Ref. [79]).

The DFT results on activation barriers of relevant atomic events are obtained by means of VASP code [81, 82] using the Perdew–Wang 1991 version of generalized gradient approximation (GGA) [83]. The spin interpolation proposed by Vosko et al., [84] is exploited to describe electronic exchange, correlation, and spin polarization. For our calculations we have used ultra-soft pseudopotentials [85, 86]. The bulk lattice constant of Pd has been found to be 3.965 Å. The Fermi-level smearing approach of Methfessel and Paxton [87] with a Gaussian width of 0.2 eV has been employed for electronic states near the Fermi level. The slab in our calculations has been constructed of seven layers and 140 Pd atoms in the periodic supercell. Four bottom layers have been kept fixed at their bulk positions, and the height of the vacuum region has been chosen to be 10 Å. We have considered that the optimized atomic geometries are achieved if the forces are smaller than 0.01 eV/Å. The calculations have been performed using a $2 \times 2 \times 1$ mesh in the Brillouin zone. The $3 \times 3 \times 1$ mesh has been also tested, however no significant changes in the results have been detected. Local density approximation (LDA) for exchange-correlation functional has been tested, but no crucial difference in the results obtained within GGA and LDA has been found.

We have involved the nudged elastic band method [88, 89] for the computation of diffusion barriers of various atomic events using VASP code. This is an efficient method for finding the minimum energy path between a given initial and final positions of an adatom during diffusion process. The diffusion path is represented by a discrete set of images connecting the initial and final positions. Adjacent images are connected by springs, mimicking an elastic band and the tangent of the path is estimated on each image [88, 89]. As a rule, the minimization of the forces acting on the images brings the band to the minimal energy path, and allows one to estimate the magnitude of activation barrier from the first principles [88, 89].

Before we proceed to the results, one important point must be discussed. An atomic process characterized by the diffusion barrier E_D can be either operative or suppressed depending on the experimental conditions (temperature T and flux F). Let us consider that $T = 290$ K and $F = 0.005$ ML/s (typical experimental parameters [6]). The deposition regime examined within out study is characterized by a typical coverage $D \sim 0.01$ ML. Therefore, the characteristic time scale t_c of the growth process is $D/F \sim 2$ s. The activation time of the atomic process t_D can be estimated using the expression $t_D \sim \nu_0^{-1} \exp(E_D/k_B T)$, where $\nu_0 = 10^{12}$ Hz is the prefactor, $k_B = 0.086$ meV/K is the Boltzmann constant, and E_D is the diffusion barrier of the atomic event. The considered event is operative only if

$t_D < t_c$, otherwise it is suppressed. All atomic processes having activation barriers $E_D > E_{cr} = 0.71$ eV are inhibited at $T = 290$ K and $F = 0.005$ ML/s. The threshold value E_{cr} depends on T (E_{cr} decreases with decreasing of T) and flux F (E_{cr} increases with decreasing of F). During our study, we compare the energy barriers of all atomistic processes with the threshold barrier (0.71 eV for this section) and determine, whether the event is operative or suppressed.

It is important to note that there is a logarithmic dependence of the magnitude of the threshold value E_{cr} on the prefactor v_0. This is a significant issue, since the magnitude of v_0 is not known exactly, and it might be easily a factor of 2 smaller or larger [90]. Due to the logarithmic dependence, E_{cr} is only slightly sensitive to the possible variations of v_0. For example, if $v_0 = 2 \times 10^{12}$ Hz, $E_{cr} = 0.725$ eV, while if $v_0 = 0.5 \times 10^{12}$ Hz, $E_{cr} = 0.69$ eV. Thus the conclusions of our study are not sensitive to the magnitude of v_0, which is chosen for the estimation of E_{cr}.

First we analyze diffusion of a single Fe adatom on a Pd(110) surface. Our studies demonstrate that it is strongly anisotropic. The activation energy for migration along the [1–10] direction is $E_1 = 0.30$ eV (Fig. 1a), while in the perpendicular (i.e., [001]) direction it is 1.57 eV (not shown in Fig. 1). At RT the adatom easily overcomes the first barrier, while the second transition is suppressed. We also note that incorporation of a Fe adatom into the topmost substrate layer (Fig. 1a and b) is possible. It takes place with the barrier of $E_2 = 0.32$ eV and decreases the energy of the system by 0.34 eV. Since the barriers E_1 and E_2 have close values and incorporation of Fe leads to the energy gain, the deposited species expel Pd atoms and embed shortly after landing.

The following point needs to be clarified next: whether or not embedded Fe atoms coalescence into compact structures within the topmost substrate layer? We have computed the binding energy of an embedded Fe dimer oriented along the [1–10] direction. This energy is found to be repulsive (0.20 eV). Thus, the buried Fe atoms repel each other, forming a disperse array within the surface layer. After incorporation, Fe species are excluded from the process of formation of the ad-layer structure.

Now we discuss the behavior of expelled Pd atoms. The diffusion barrier of a Pd adatom on Pd(110) along the [1–10] direction is 0.45 eV. Such atomic event takes place at RT. The barrier for the direct hop along the [001] direction is 1.26 eV, and such event is suppressed. However in contrast to Fe atoms, a Pd atom can migrate along the [001] direction with a barrier of 0.54 eV via exchange with one of Pd atoms of the topmost layer. Not all hollow sites are energetically equal for the Pd adatom: adsorption positions in the vicinity of embedded Fe atoms (Fig. 1b) are the preferable ones. When the Pd adatom is located near an embedded Fe, the energy gain is 0.05 eV (Fig. 1b and c). But this energy is too small to bind together the expelled Pd and the embedded Fe atom at RT; thus, the Pd atom follows 2D random diffusion along the surface.

Figure 2a–c depicts the evolution of a small Pd aggregate. The most stable configuration of two Pd adatoms is a dimer, oriented along the [1–10] direction on top of an embedded Fe atom. We note that at RT the aggregation of Pd dimers not necessarily takes place in the vicinity of the buried Fe species. Since the binding energy of an embedded Fe atom and a Pd adatom is quite small (0.05 eV, Fig. 1c), nucleation of Pd can start at any place of a surface with non-zero probability. When the third Pd atom approaches the dimer, the formation of a linear chain is energetically favorable (Fig. 2b). With the arriving of the forth Pd adatom, the length of the chain increases (Fig. 2c).

The shape of nanostructures growing on a (110) surface is determined by the interplay between the diffusion barriers for attachment and detachment to an aggregate [75–77]. With increasing temperature T at a fixed flux F the system

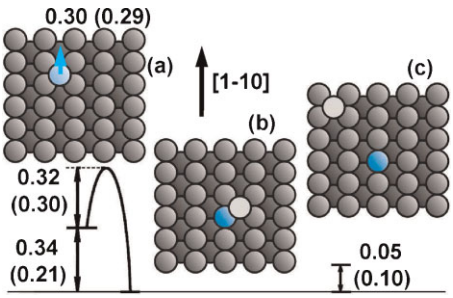

Figure 1 (online color at: www.pss-b.com) Top view of the surface model, showing the first phase of Fe/Pd(110) and Co/Cu(110) interface formation. Gray (light-gray) circles represent Pd or Cu atoms of the substrate (of the first ad-layer). Blue circles correspond to Fe or Co atoms. The relative energies between atomic configurations (in eV) and activation barriers (in eV) are presented. (a) A Fe (Co) adatom is on a Pd(110) (Cu(110)) surface. (b) The embedded Fe (Co) atom and the substituted Pd (Cu) adatom nearby. (c) The expelled Pd (Cu) adatom is located far from the embedded Fe (Co) atom [74, 79].

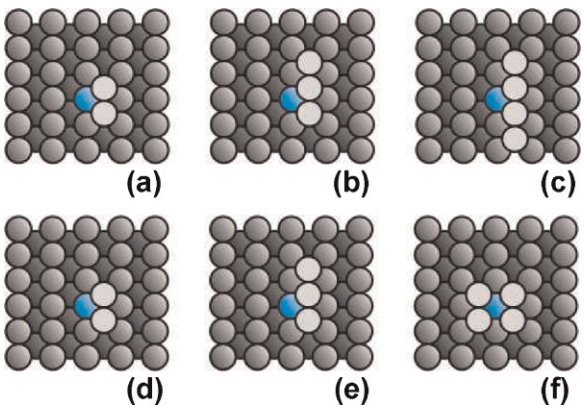

Figure 2 (online color at: www.pss-b.com) Initial stages of growth of small Pd aggregates on Pd(110) during deposition of Fe (a–c) and of small Cu aggregates on Cu(110) during epitaxy of Co (d–f). The most stable configurations of two, three, and four expelled Pd and Cu atoms are demonstrated. The colors are the same as in Fig. 1 [74, 79].

follows through three basic growth modes: (i) small aggregates at low T; (ii) atomic chains oriented along the [1–10] direction at intermediate T (when T is not enough to break in-channel adatom-adatom bond); and (iii) 2D anisotropic islands elongated along the [1–10] direction at high T. The relevant diffusion events for a Pd adatom in the vicinity of a Pd chain and their activation energies are shown in Fig. 3. The Pd adatom migrates along the wire with a barrier of 0.52 eV and detaches itself from it with the barrier of 0.49 eV. These events are operative at RT. At the same time, the energy for breaking the in-channel Pd–Pd bond is 0.73 eV. This transition is mainly suppressed at RT. Thus according to the results of Refs. [75–77], at RT we expect growth of Pd chains along the [1–10] direction.

In order to prove this suggestion and to reveal the morphology of Pd(110) after deposition of Fe atoms, we employ kMC simulations. The kMC model [80] describes epitaxial growth in terms of rates of elementary stochastic processes (deposition, surface diffusion, and detachment/attachment from/to a chain or a nanoisland). The rate of an atomic event is computed using the Arrhenius expression $v = v_0 \exp(-E_D/k_B T)$, where $v_0 = 10^{12}$ Hz is the prefactor, E_D is the activation barrier, and k_B is the Boltzmann constant. During recent years this model has been widely applied for studying atomic self-organization during homo- and hetero-epitaxy [75, 76, 91–99]. Our kMC simulations are carried out on a (110) lattice consisting of 142×200 atoms ($56 \times 56\,nm^2$). Periodic boundary conditions are applied in the surface plane. Figure 4a demonstrates the morphology of a Pd(110) surface exposed to 0.12 ML of Fe atoms at RT ($F = 0.005$ ML/s). Growth of randomly distributed monatomic chains elongated along the [1–10] direction is observed. The atomic-scale resolution (Fig. 4b) shows that almost all deposited Fe atoms are confined within the topmost substrate layer, while the ad-layer structure consists of Pd atoms. The average length of a wire is about 30 atoms. This is consistent with the experimental observations: self-assembly of atomic chains with an average length of about 25 atoms has taken place at coverage of ~0.15 ML [6].

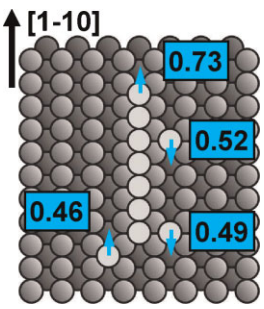

Figure 3 (online color at: www.pss-b.com) Atomic events responsible for the growth of Pd chains elongated along the [1–10] direction. Gray and light-gray circles show Pd atoms of the topmost surface layer and in the ad-layer position, respectively. The activation barriers are given in eV [79].

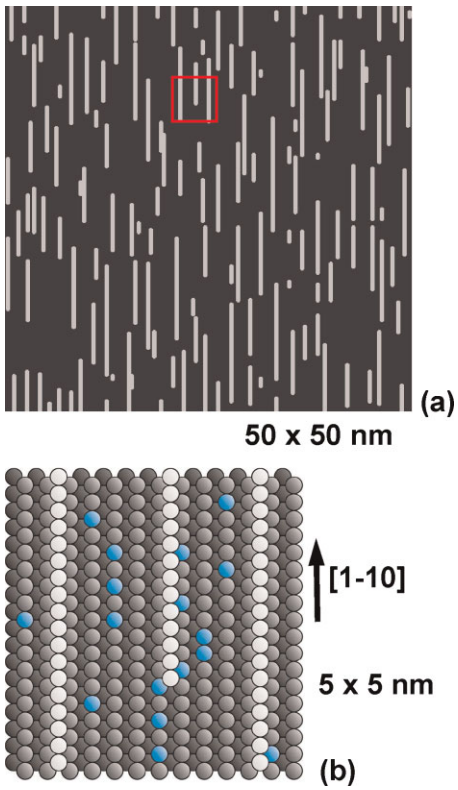

Figure 4 (online color at: www.pss-b.com) (a) Top view of a Pd(110) surface exposed by about 0.12 ML of Fe atoms at 290 K: the result of the kMC simulations. (b) An atomic-scale view of the area, marked in (a) with the red rectangle. Gray (light-gray) circles represent Pd atoms of the surface (the first ad-layer). Blue circles correspond to Fe atoms embedded into the surface layer [79].

One can control the average length of the chains manipulating the temperature T. Increasing T leads to the growth of the longer wires and *vice versa*. However, there is natural interval of T suitable for the fabrication of wires. At $T = 210$ K an insufficient mobility of adatoms leads only to the growth of small aggregates three to five atoms long and one to two atoms wide [79]. In this case the ad-layer structure still consists of Pd atoms, while Fe species are buried. On the other hand, at a high T (~350 K in our case) the self-assembly of 2D islands two to three atomic rows wide and consisting of expelled Pd atoms is observed [79]. This result is intuitively clear: when the Pd–Pd in-channel bond is broken (the barrier is 0.73 eV, Fig. 3), transition from 1D wires to 2D nanoislands occurs [75–77]. The experimental verification of our theoretical predictions on the growth scenario of Fe on Pd(110) and Co on Pd(110) has been performed recently [100]. Electronic structure measurements by means of scanning tunneling spectroscopy over self-assembled monatomic wires have demonstrated that in the sub-monolayer regime they indeed consist of Pd atoms.

Due to the fact that Fe atoms incorporate into the substrate shortly after landing and are further excluded from the formation of the ad-layer structure, there is no qualitative

difference between growth of Fe/Pd(110), Co/Pd(110), and Pd/Pd(110) at low coverage (∼0.1–0.2 ML). Thus, the results of our calculations shed a light on the recent experiments on TD of Co on Pd(110) [6]. It has been believed that at low coverage (∼0.15 ML) the growth of Co chains takes place. However, our simulations demonstrate that this is not quite correct: Co atoms incorporate into the substrate forming a randomly distributed array of individual atoms, while the ad-layer structure consist mainly of Pd atoms. When the coverage increases, the incorporation of Co atoms is suppressed, since the barrier for exchange of a Co adatom next to already embedded Co atoms becomes high, 0.60 eV (0.79 eV in LDA). Hence above the coverage of $\gtrsim$0.5 ML, Co atoms contribute remarkably to the ad-layer structure, i.e., nanostripes (Fig. 2b in Ref. [6]). Thus the MOKE signal measured for 0.5 ML of Co on Pd(110) [6] relates to the Co-nanostripes on Pd(110) grown around and on top of Pd wires and reflects their magnetic anisotropy.

3 Co on Cu(110) In this section we discuss the self-assembly of Co atoms on Cu(110) at RT. First we present the results of calculations of activation barriers of relevant atomic events. Then we turn to the large-scale atomic simulations by means of kMC method in order to demonstrate the structure of the interface in the examined system.

Distinctly from the case of Fe/Pd(110) (see previous section), activation barriers of basic atomic events are computed by means of quenched molecular dynamics (QMD) calculations with *ab initio* based interatomic Co–Cu potentials formulated in the second moment of the tight-binding approximation [101, 102]. Nevertheless, we compare some of these barriers with the results of the DFT calculations (performed using VASP code [73, 74]), to be sure that the exploited many-body potentials give correct values. Previous studies have demonstrated that the combination of *ab initio* and tight-binding methods allows one to construct many-body potentials for low-dimensional structures and to study systems of hundreds and thousands of atoms in fully relaxed geometries [103–108]. The parameters of our potentials are given in Ref. [109]. Our QMD simulations are carried out in a finite slab of ten layers, where each layer contains 1260 atoms. Four bottom layers are fixed, and periodic boundary conditions are applied in the surface plane.

The quenching procedure consists in the solving of the Newton equations of motion for each atom $\boldsymbol{F}_i(t) = m\,\mathrm{d}\boldsymbol{v}_i/\mathrm{d}t$ and canceling $\boldsymbol{v}_i$ when the product $\boldsymbol{F}_i(t)\boldsymbol{v}_i(t)$ is negative [110]. To compute an activation barrier, the quenching has to be done with the adatom at the hollow site and at the saddle point. The saddle point is found by evaluating the energy for many different positions along the diffusion coordinate [110]. As at the saddle point at least one coordinate is unstable, it is fixed to prevent the adatom coming back to the position with a minimum energy.

The quantitative comparison between the results calculated from the first principles (or measured experimentally) and those obtained using the tight-binding-based interatomic potentials for a system of Cu and Co atoms has been performed in the previous studies. The details can be found in Refs. [111, 112]. For example, it has been shown that the employed many-body potentials nicely reproduce bulk properties (lattice constant, cohesive energy, bulk modulus, and elastic constants) of Cu and Co crystals measured in the experiments (see Table I in Ref. [111]). There is a good agreement between the *ab initio* calculated solution energy of a single Co impurity in the bulk of Cu and that computed by means of the potentials [111]. The employed potentials also reproduce binding energies of small supported and embedded Co clusters on two types of surfaces, Cu(100) [111] and Cu(111) [112]. Therefore, we are convinced that our potentials are well suited for the large-scale atomic simulation in the examined system.

In the following we concentrate on the basic atomic events driving the epitaxial growth of Co on Cu(110). We find that a Co adatom on Cu(110) (Fig. 1a) diffuses along the [1–10] direction with the barrier of $E_1 = 0.29$ eV. At RT a Co adatom overcomes this barrier. The corresponding value computed by means of VASP code [81, 82] in GGA approximation is 0.35 eV [74]. Similar to the case of Fe/Pd(110), diffusion of Co on Cu(110) is strongly anisotropic: the barrier for migration along the [001] direction exceeds 1.0 eV, and such motion is suppressed. Incorporation of a Co adatom into the topmost substrate layer (Fig. 1b) decreases the total energy of the system by $\Delta E = 0.21$ eV (VASP gives 0.22 eV [74]) and takes place with a barrier E_2 of 0.30 eV (VASP gives 0.32 eV [74]). Since the barriers E_1 and E_2 have close values and incorporation of Co leads to the energy gain, deposited species embed into the substrate shortly after landing, similar to Fe and Co adatoms on Pd(110).

Substituted Cu atoms exhibit 2D random walks on a surface. To prove this statement we analyze diffusion of Cu adatoms on Cu(110). The barrier for migration along the [1–10] direction is 0.26 eV (VASP gives 0.32 eV [73]). Cu atoms migrate along the [001] direction via exchange with one of Cu atoms of the topmost layer with the barrier 0.30 eV (VASP gives 0.35 eV [73]). It is worth to note that there are preferable adsorption positions for diffusing Cu atoms: hollow sites atop buried Co atoms (Fig. 1b). When a Cu adatom is located near an embedded Co atom, the energy gain is 0.10 eV (Fig. 1c). Migrating Cu atoms coalescence into small aggregates (dimers, trimers), and such nucleation is energetically more favorable atop of embedded Co species.

Now we turn to the evolution of a small Cu aggregates. Two Cu atoms form a dimer, oriented along the [1–10] direction above an embedded Co atom (Fig. 2d). If the third Cu atom approaches, a linear chain is the most stable configuration (Fig. 2e). When four Cu atoms are nucleated, formation of the stable cluster "two-by-two" takes place (Fig. 2f). To explain the driving force behind this phenomenon, we note that the interaction between Co–Cu is profoundly stronger than the interaction between Cu–Cu [113]. As the result, an embedded Co atom acts as a pinning

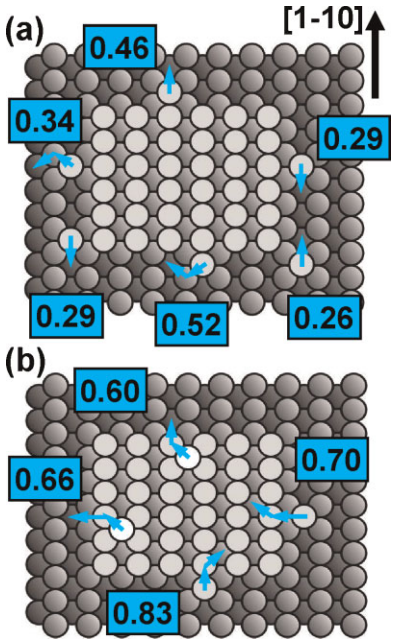

Figure 5 (online color at: www.pss-b.com) (a) Basic atomic events responsible for the growth of Cu nanoislands elongated along the [1–10] direction on Cu(110). (b) Interlayer mass transport at the edges of a nanoisland. Gray (light-gray, light–light gray) circles represent Cu atoms of the surface (the first ad-layer, the second ad-layer). The activation barriers are given in eV [74].

center for expelled Cu atoms. This finding is similar to those reported in Refs. [50, 113, 114] for Co on Cu(100).

Next we examine diffusion of a Cu adatom on Cu(110) in the vicinity of a Cu nanoisland, which determines the shape of surface nanostructures. A Cu adatom migrates along the [1–10] direction along the edge of a nanoisland with the barrier of 0.29 eV (Fig. 5a). The same energy is required to detach the nanoisland at the corner. The barrier for the breaking of the in-channel Cu–Cu bond is 0.46 eV, while the step edge diffusion along the [001] direction requires the energy of 0.52 eV (Fig. 5a). Evidently, all these barriers are not so high, and thus all atomic events presented on Fig. 5a are operative at RT. In such situation, one can expect growth of Cu islands elongated along the [1–10] direction [75].

With increasing the coverage, the size of growing nanoislands increases, and new deposited Co atoms land atop them with a non-zero probability, forming the second ad-layer. Such Co atoms follow the process shown in Fig. 1a and b: they embed into the first ad-layer in the vicinity of the place of landing and substitute one of Cu atoms. The expelled Cu atoms exhibit 2D random walks atop the island (on the second ad-layer) and approach its edges. To understand the behavior of such atoms, atomic interlayer mass transport at the edge of a nanoisland must be carefully studied. The downward mass transport of Cu atoms (from the second to the first ad-layer) is induced with the barrier 0.60 eV if Cu atoms are located near the step edge parallel to the [001] direction, and with the barrier 0.66 eV if they are at the edge parallel to the [1–10] direction (Fig. 5b). The opposite transitions occur with the barriers 0.83 and 0.70 eV, respectively. All these four barriers are quite high. Thus, the probability of the interlayer mass transport strongly depends on the deposition rate F. When F is large enough, Cu atoms diffusing atop a nanoisland do not have enough time to induce downward mass transport to the first ad-layer, and the 3D growth mode prevails.

Since all main atomic events responsible for the RT epitaxial growth of Co on Cu(110) have been discussed, now we turn to the kMC simulations of the self-organization of surface nanostructures in this system. The kMC studies are carried out on a close-packed (110) lattice consisting of 166×234 atoms ($60 \times 60\,\mathrm{nm}^2$), and periodic boundary conditions are applied in the surface plane. The parameters of the system are chosen to be close to the experimental setup of Hope et al. [70]: $F = 0.01$ ML/s, $T = 290$ K. Figure 6a shows the morphology of Cu(110) covered by about 0.07 ML of Co atoms. Formation of 1 ML high randomly distributed nanoislands, elongated along the [1–10] direction, takes place. The atomic-scale resolution (Fig. 6b) indicates a strong intermixing between deposited and substrate atoms and shows that nanoislands consist of Cu atoms. Figure 7a

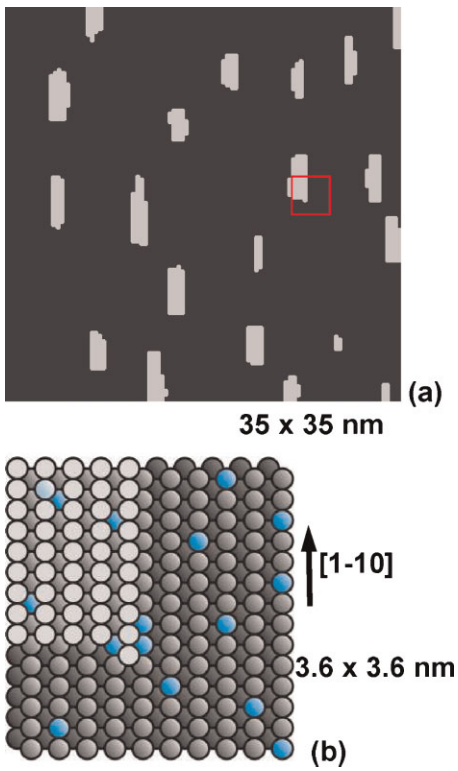

Figure 6 (online color at: www.pss-b.com) (a) The morphology of a Cu(110) surface exposed by about 0.07 ML of Co atoms at 290 K: the kMC simulation. (b) An atomic-scale view of the area, marked in (a) with the red rectangle. Gray (light-gray, white) circles represent Cu atoms of the surface (the first, the second ad-layer). Blue (pale-blue) circles correspond to Co atoms embedded into the surface layer (in the first ad-layer) [74].

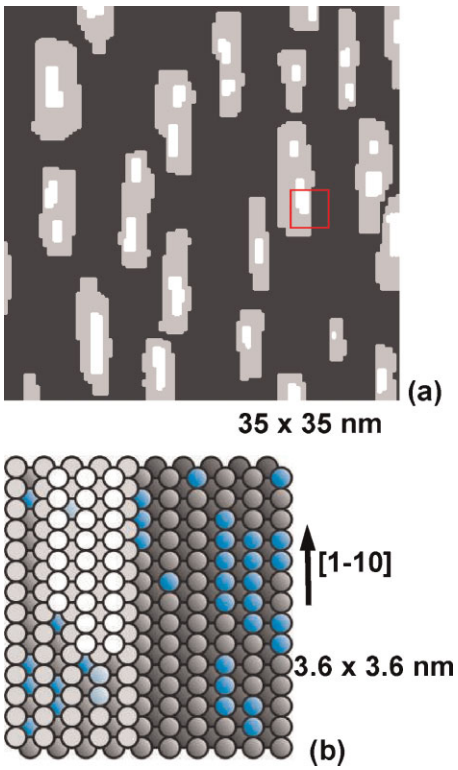

Figure 7 (online color at: www.pss-b.com) (a) The morphology of a Cu(110) surface exposed by about 0.45 ML of Co atoms at 290 K: the kMC simulation. (b) An atomic-scale view of the area, marked in (a) with the red rectangle. The colors are the same as in Fig. 6 [74].

presents the morphology of Cu(110) covered by about 0.45 ML of Co atoms. Nanoislands have now larger lateral sizes and become 2 ML high. The atomic-scale resolution (Fig. 7b) indicates that the second ad-layer consists of Cu atoms, and a small fraction of Co atoms appears within the first ad-layer.

Our results provide a deeper understanding of recent experimental studies. It has been reported on the paramagnetism of thin films, surprisingly observed during early stages of epitaxial growth of Co on Cu(110) [70]. Figures 6 and 7 indicate that two factors could quench the magnetic signal of Co deposited on Cu(110): (i) Co atoms are incorporated into the non-magnetic substrate and part of them are covered by expelled Cu atoms; (ii) embedded Co species form Co clusters of few atoms, which could exhibit superparamagnetic behavior due to their small sizes.

4 Conclusions We have examined the atomic scale RT self-organization of 3d magnetic atoms (Fe, Co) on fcc (110) non-magnetic substrates (Cu(110), Pd(110)). It has been revealed that the interface intermixing dominates on the early stages of heteroepitaxy. Our results for Fe/Pd(110) and Co/Pd(110) have indicated that in these systems deposited species incorporate into the topmost substrate layer and form disordered arrays within it. At the same time, the expelled Pd atoms diffuse on a surface and aggregate into monatomic chains at the coverages of <0.2 ML. The simulations for Co/Cu(110) have shown that embedded Co atoms serve as nucleation centers for substituted Cu atoms. Surface diffusion of expelled Cu adatoms causes an elongated along the [1–10] direction shape of nanoislands consisting mainly of Cu atoms. The results of our studies give a deeper understanding of recent experimental investigations of heteroepitaxial growth on fcc (110) surfaces.

Acknowledgements We are gratefully acknowledging the financial support of Deutsche Forschungsgemeinschaft (SPP1153).

References

[1] J. V. Barth, G. Costantini, and K. Kern, Nature (London) **437**, 671 (2005).
[2] P. Gambardella, M. Blanc, L. Bürgi, K. Kuhnke, and K. Kern, Surf. Sci. **449**, 93 (2000).
[3] P. Gambardella, M. Blanc, H. Brune, K. Kuhnke, and K. Kern, Phys. Rev. B **61**, 2254 (2000).
[4] P. Gambardella, A. Dallmeyer, K. Maiti, M. C. Malagoli, W. Eberhardt, K. Kern, and C. Carbone, Nature (London) **416**, 301 (2002).
[5] S. Shiraki, H. Fujisawa, T. Nakamura, T. Muro, M. Nantoh, and M. Kawai, Phys. Rev. Lett. **92**, 096102 (2004).
[6] L. Yan, M. Przybylski, Y. F. Lu, W. H. Wang, J. Barthel, and J. Kirschner, Appl. Phys. Lett. **86**, 102503 (2005).
[7] Y. Mo, K. Varga, E. Kaxiras, and Z. Zhang, Phys. Rev. Lett. **94**, 155503 (2005).
[8] J. Guo, Y. Mo, E. Kaxiras, Z. Zhang, and H. H. Weitering, Phys. Rev. B **73**, 193405 (2006).
[9] H. F. Ding, V. S. Stepanyuk, P. A. Ignatiev, N. N. Negulyaev, L. Niebergall, M. Wasniowska, C. L. Gao, P. Bruno, and J. Kirschner, Phys. Rev. B **76**, 033409 (2007).
[10] Y. Pennec, W. Auwärter, A. Schiffrin, A. Weber-Bargioni, A. Riemann, and J. V. Barth, Nature Nanotechnol. **2**, 99 (2007).
[11] A. Schiffrin, J. Reichert, W. Auwärter, G. Jahnz, Y. Pennec, A. Weber-Bargioni, V. S. Stepanyuk, L. Niebergall, P. Bruno, and J. V. Barth, Phys. Rev. B **78**, 035424 (2008).
[12] C. Liu, T. Uchihashi, and T. Nakayama, Phys. Rev. Lett. **101**, 146104 (2008).
[13] H. J. Elmers, J. Hauschild, H. Höche, U. Gradmann, H. Bethge, D. Heuer, and U. Köhler, Phys. Rev. Lett. **73**, 898 (1994).
[14] J. Shen, R. Skomski, M. Klaua, H. Jenniches, S. S. Manoharan, and J. Kirschner, Phys. Rev. B **56**, 2340 (1997).
[15] J. Shen, M. Klaua, P. Ohresser, H. Jenniches, J. Barthel, Ch. V. Mohan, and J. Kirschner, Phys. Rev. B **56**, 11134 (1997).
[16] G. Brown, H. K. Lee, T. C. Schulthess, B. Ujfalussy, G. M. Stocks, W. H. Butler, D. P. Landau, J. P. Pierce, J. Shen, and J. Kirschner, J. Appl. Phys. **91**, 7056 (2002).
[17] J. Shen, J. P. Pierce, E. W. Plummer, and J. Kirschner, J. Phys.: Condens. Matter **15**, R1 (2003).
[18] F. J. Himspel, J. E. Ortega, G. J. Mankey, and R. F. Willis, Adv. Phys. **47**, 511 (1998).
[19] S. Shiraki, H. Fujisawa, T. Nakamura, T. Muro, M. Nantoh, and M. Kawai, Phys. Rev. B **78**, 115428 (2008).

[20] X.-D. Ma, D. I. Bazhanov, O. Fruchart, F. Yildiz, T. Yokoyama, M. Przybylski, V. S. Stepanyuk, W. Hergert, and J. Kirschner, Phys. Rev. Lett. **102**, 205503 (2009).
[21] C. Tegenkamp, J. Phys.: Condens. Matter **21**, 013002 (2009).
[22] H. Brune, H. Röder, C. Boragno, and K. Kern, Phys. Rev. Lett. **73**, 1955 (1994).
[23] K. Bromann, H. Brune, H. Röder, and K. Kern, Phys. Rev. Lett. **75**, 677 (1995).
[24] H. Brune, M. Giovannini, K. Bromann, and K. Kern, Nature (London) **394**, 451 (1998).
[25] J. E. Prieto, J. de la Figuera, and R. Miranda, Phys. Rev. B **62**, 2126 (2000).
[26] I. Chado, C. Goyhenex, H. Bulou, and J. P. Bucher, Phys. Rev. B **69**, 085413 (2004).
[27] H. Bulou, F. Scheurer, P. Ohresser, A. Barbier, S. Stanescu, and C. Quirós, Phys. Rev. B **69**, 155413 (2004).
[28] M. V. Rastei, J. P. Bucher, P. A. Ignatiev, V. S. Stepanyuk, and P. Bruno, Phys. Rev. B **75**, 045436 (2007).
[29] M. Bachmann, M. Gabl, C. Deisl, N. Memmel, and E. Bertel, Phys. Rev. B **78**, 235410 (2008).
[30] M. Gabl, M. Bachmann, N. Memmel, and E. Bertel, Phys. Rev. B **79**, 153409 (2009).
[31] Y. Qiang, R. F. Sabiryanov, S. S. Jaswal, Y. Liu, H. Haberland, and D. J. Sellmyer, Phys. Rev. B **66**, 064404 (2002).
[32] J. P. Pierce, M. A. Torija, Z. Gai, J. Shi, T. C. Schulthess, G. A. Farnan, J. F. Wendelken, E. W. Plummer, and J. Shen, Phys. Rev. Lett. **92**, 237201 (2004).
[33] M. A. Torija, A. P. Li, X. C. Guan, E. W. Plummer, and J. Shen, Phys. Rev. Lett. **93**, 257203 (2005).
[34] S. Rohart, V. Repain, A. Tejeda, P. Ohresser, F. Scheurer, P. Bencok, J. Ferrer, and S. Rousset, Phys. Rev. B **73**, 165412 (2006).
[35] R. Skomski, J. Zhang, V. Sessi, J. Honolka, A. Enders, and K. Kern, J. Appl. Phys. **103**, 07D519 (2008).
[36] Y. Nahas, V. Repain, C. Chacon, Y. Girard, J. Lagoute, G. Rodary, J. Klein, S. Rousset, H. Bulou, and C. Goyhenex, Phys. Rev. Lett. **103**, 067202 (2009).
[37] J. Tersoff, Phys. Rev. Lett. **74**, 434 (1995).
[38] J. N. Andersen, E. Lundgren, R. Nyholm, and M. Qvarford, Phys. Rev. Lett. **46**, 12784 (1992).
[39] D. D. Chambliss, R. J. Wilson, and S. Chiang, J. Vac. Sci. Technol. A **10**, 1993 (1992).
[40] P. T. Sprunger, E. Lægsgaard, and F. Besenbacher, Phys. Rev. B **54**, 8163 (1996).
[41] H. W. Sheng and E. Ma, Phys. Rev. B **61**, 9979 (2000).
[42] S.-L. Chang, J.-M. Wen, P. A. Thiel, S. Günther, J. A. Meyer, and R. J. Behm, Phys. Rev. B **53**, 13747 (1996).
[43] F. Patthey, C. Massobrio, and W.-D. Schneider, Phys. Rev. B **53**, 13146 (1996).
[44] B. Müller, L. Nedelmann, B. Fischer, H. Brune, J. V. Barth, and K. Kern, Phys. Rev. Lett. **80**, 2642 (1998).
[45] J. Lindner, P. Poulopoulos, F. Wilhelm, M. Farle, and K. Baberschke, Phys. Rev. B **62**, 10431 (2000).
[46] H. L. Meyerheim, D. Sander, N. N. Negulyaev, V. S. Stepanyuk, R. Popescu, I. Popa, and J. Kirschner, Phys. Rev. Lett. **100**, 146101 (2008).
[47] K. E. Johnson, D. D. Chambliss, R. J. Wilson, and S. Chiang, J. Vac. Sci. Technol. A **11**, 1654 (1993).
[48] D. D. Chambliss and K. E. Johnson, Phys. Rev. B **50**, 5012 (1994).
[49] J. Fassbender, R. Allenspach, and U. Dürig, Surf. Sci. Lett. **383**, L742 (1997).
[50] F. Nouvertné, U. May, M. Bamming, A. Rampe, U. Korte, G. Güntherodt, R. Pentcheva, and M. Scheffler, Phys. Rev. B **60**, 14382 (1999).
[51] M. M. J. Bischoff, T. Yamada, A. J. Quinn, R. G. P. van der Kraan, and H. van Kempen, Phys. Rev. Lett. **87**, 246102 (2001).
[52] R. M. Tromp, Phys. Rev. B **47**, 7125 (1993).
[53] R. M. Tromp, A. W. Denier van der Gon, and M. C. Reuter, Phys. Rev. Lett. **68**, 2313 (1992).
[54] A. A. Stekolnikov, F. Bechstedt, M. Wisniewski, J. Schäfer, and R. Claessen, Phys. Rev. Lett. **100**, 196101 (2008).
[55] D. E. P. Vanpoucke and G. Brocks, Phys. Rev. B **77**, 241308R (2008).
[56] C. Stampfl, M. Scheffler, H. Over, J. Burchhardt, M. Nielsen, D. L. Adams, and W. Moritz, Phys. Rev. Lett. **68**, 94 (1992).
[57] J. Neugebauer and M. Scheffler, Phys. Rev. Lett. **71**, 577 (1993).
[58] H. Röder, R. Shuster, H. Brune, and K. Kern, Phys. Rev. Lett. **71**, 2086 (1993).
[59] J. S. Tsay, Y. D. Yao, and C. S. Shern, Phys. Rev. B **58**, 3609 (1998).
[60] S. Oppo, V. Fiorentini, and M. Scheffler, Phys. Rev. Lett. **71**, 2437 (1993).
[61] J. Jacobsen, L. Pleth Nielsen, F. Besenbacher, I. Stensgaard, E. Lægsgaard, T. Rasmussen, K. W. Jacobsen, and J. K. Nørskov, Phys. Rev. Lett. **75**, 489 (1995).
[62] H. Oughaddou, S. Sawaya, J. Goniakowski, B. Aufray, G. Le Lay, J. M. Gay, G. Tréglia, J. P. Bibérian, N. Barrett, C. Guillot, A. Mayne, and G. Dujardin, Phys. Rev. B **62**, 16653 (2000).
[63] L. Gómez, C. Slutzky, J. Ferrón, J. de la Figuera, J. Camarero, A. L. Vázquez de Parga, J. J. de Miguel, and R. Miranda, Phys. Rev. Lett. **84**, 4397 (2000).
[64] L. Pleth Nielsen, F. Besenbacher, I. Stensgaard, E. Lægsgaard, C. Engdahl, P. Stoltze, K. W. Jacobsen, and J. K. Nørskov, Phys. Rev. Lett. **71**, 754 (1993).
[65] O. Kizilkaya, D. A. Hite, W. Zhao, P. T. Sprunger, E. Lægsgaard, and F. Besenbacher, Surf. Sci. **596**, 242 (2005).
[66] H. Röder, E. Hahn, H. Brune, J.-P. Bucher, and K. Kern, Nature (London) **366**, 141 (1993).
[67] M. Guillope and B. Legrand, Surf. Sci. **215**, 577 (1989).
[68] E. Hahn, E. Kampshoff, A. Fricke, J.-P. Bucher, and K. Kern, Surf. Sci. **319**, 277 (1994).
[69] Y. Li, M. C. Bartelt, J. W. Evans, N. Waelchli, E. Kampshoff, and K. Kern, Phys. Rev. B **56**, 12539 (1997).
[70] S. Hope, M. Tselepi, E. Gu, T. M. Parker, and J. A. C. Bland, J. Appl. Phys. **85**, 6094 (1999).
[71] S. M. York and F. M. Leibsle, Phys. Rev. B **64**, 033411 (2001).
[72] C. Massobrio and P. Fernandez, J. Chem. Phys. **102**, 605 (1995).
[73] R. Sathiyanarayanan and T. L. Einstein, Surf. Sci. **603**, 2387 (2009).
[74] O. V. Stepanyuk, N. N. Negulyaev, A. M. Saletsky, and W. Hergert, Phys. Rev. B **78**, 113406 (2008).
[75] R. Ferrando, F. Hontinfinde, and A. C. Levi, Phys. Rev. B **56**, R4406 (1997).
[76] R. Ferrando, F. Hontinfinde, and A. C. Levi, Surf. Sci. **402–404**, 286 (1998).

[77] C. Mottet, R. Ferrando, F. Hontinfinde, and A. C. Levi, Surf. Sci. **417**, 220 (1998).
[78] A. Videcoq, F. Hontinfinde, and R. Ferrando, Surf. Sci. **515**, 575 (2002).
[79] O. V. Stepanyuk, N. N. Negulyaev, P. A. Ignatiev, M. Przybylski, W. Hergert, A. M. Saletsky, and J. Kirschner, Phys. Rev. B **79**, 155410 (2009).
[80] K. A. Fichthorn and W. H. Weinberg, J. Chem. Phys. **95**, 1090 (1991).
[81] G. Kresse and J. Hafner, Phys. Rev. B **47**, 558 (1993).
[82] G. Kresse and J. Furthmüller, Phys. Rev. B **54**, 11169 (1996).
[83] J. P. Perdew and Y. Wang, Phys. Rev. B **45**, 13244 (1992).
[84] S. H. Vosko, L. Wilk, and M. Nusair, Can. J. Phys. **58**, 1200 (1980).
[85] D. Vanderbilt, Phys. Rev. B **41**, 7892 (1990).
[86] G. Kresse and J. Hafner, J. Phys.: Condens. Matter **6**, 8245 (1994).
[87] M. Methfessel and A. T. Paxton, Phys. Rev. B **40**, 3616 (1989).
[88] G. Mills and H. Jonsson, Phys. Rev. Lett. **72**, 1124 (1993).
[89] G. Mills, H. Jonsson, and G. K. Schenter, Surf. Sci. **324**, 305 (1995).
[90] N. Knorr, H. Brune, M. Epple, A. Hirstein, M. A. Schneider, and K. Kern, Phys. Rev. B **65**, 115420 (2002).
[91] S. Ovesson, A. Bogicevic, and B. I. Lundqvist, Phys. Rev. Lett. **83**, 2608 (1999).
[92] S. Ovesson, A. Bogicevic, G. Wahnström, and B. I. Lundqvist, Phys. Rev. B **64**, 125423 (2001).
[93] K. A. Fichthorn and M. Scheffler, Phys. Rev. Lett. **84**, 5371 (2000).
[94] K. A. Fichthorn, M. L. Merrick, and M. Scheffler, Phys. Rev. B **68**, 041404R (2003).
[95] M. Müller, K. Albe, C. Busse, A. Thoma, and T. Michely, Phys. Rev. B **71**, 075407 (2005).
[96] E. Cox, M. Li, P.-W. Chung, C. Ghosh, T. S. Rahman, C. J. Jenks, J. W. Evans, and P. A. Thiel, Phys. Rev. B **71**, 115414 (2005).
[97] M. Ziegler, J. Kröger, R. Berndt, A. Filinov, and M. Bonitz, Phys. Rev. B **78**, 245427 (2008).
[98] N. N. Negulyaev, V. S. Stepanyuk, L. Niebergall, P. Bruno, W. Hergert, J. Repp, K.-H. Rieder, and G. Meier, Phys. Rev. Lett. **101**, 226601 (2008).
[99] N. N. Negulyaev, V. S. Stepanyuk, L. Niebergall, P. Bruno, M. Pivetta, M. Ternes, F. Patthey, and W.-D. Schneider, Phys. Rev. Lett. **102**, 246102 (2009).
[100] D. H. Wei, C. L. Gao, Kh. Zakeri, and M. Przybylski, Phys. Rev. Lett. **103**, 225504 (2009).
[101] V. Rosato, B. Guillope, and B. Legrand, Philos. Mag. A **59**, 321 (1989).
[102] F. Cleri and V. Rosato, Phys. Rev. B **48**, 22 (1993).
[103] O. V. Lysenko, V. S. Stepanyuk, W. Hergert, and J. Kirschner, Phys. Rev. Lett. **89**, 126102 (2002).
[104] R. A. Miron and K. A. Fichthorn, Phys. Rev. Lett. **93**, 128301 (2004).
[105] K. Sastry, D. D. Johnson, D. E. Goldberg, and P. Bellon, Phys. Rev. B **72**, 085438 (2005).
[106] V. S. Stepanyuk, A. L. Klavsyuk, W. Hergert, A. M. Saletsky, P. Bruno, and I. Mertig, Phys. Rev. B **70**, 195420 (2004).
[107] S. Pick, V. S. Stepanyuk, A. L. Klavsyuk, L. Niebergall, W. Hergert, J. Kirschner, and P. Bruno, Phys. Rev. B **70**, 224419 (2004).
[108] M. V. Rastei, B. Heinrich, L. Limot, P. A. Ignatiev, V. S. Stepanyuk, P. Bruno, and J. P. Bucher, Phys. Rev. Lett. **99**, 246102 (2007).
[109] N. N. Negulyaev, V. S. Stepanyuk, P. Bruno, L. Diekhöner, P. Wahl, and K. Kern, Phys. Rev. B **77**, 125437 (2008).
[110] F. Hontinfinde, R. Ferrando, and A. C. Levi, Surf. Sci. **366**, 306 (1996).
[111] N. A. Levanov, V. S. Stepanyuk, W. Hergert, D. I. Bazhanov, P. H. Dederichs, A. Katsnelson, and C. Massobrio, Phys. Rev. B **61**, 2230 (2000).
[112] D. V. Tsivlin, V. S. Stepanyuk, W. Hergert, and J. Kirschner, Phys. Rev. B **68**, 205411 (2003).
[113] R. Pentcheva, K. A. Fichthorn, M. Scheffler, T. Bernhard, R. Pfandzelter, and H. Winter, Phys. Rev. Lett. **90**, 076101 (2003).
[114] R. Pentcheva and M. Scheffler, Phys. Rev. B **65**, 155418 (2002).